

Partial wave analyses of $J = 0^+ \rightarrow 0^0$ and $0^0 \rightarrow 0^0$

M. Ablikim¹, J. Z. Bai[†], Y. Ban¹², J. G. Bian¹, X. Cai[†], H. F. Chen¹⁷, H. S. Chen¹, H. X. Chen¹, J. C. Chen¹, Jin Chen¹, Y. B. Chen¹, S. P. Chf², Y. P. Chu¹, X. Z. Cui[†], Y. S. Dai¹⁹, L. Y. Diao⁹, Z. Y. Deng¹, Q. F. Dong¹⁵, S. X. Du¹, J. Fang¹, S. S. Fang², C. D. Fu¹, C. S. Gao¹, Y. N. Gao¹⁵, S. D. Gu¹, Y. T. Gu⁴, Y. N. Guo¹, Y. Q. Guo¹, Z. J. Guo¹⁶, F. A. Harris¹⁶, K. L. He¹, M. He¹³, Y. K. Heng¹, H. M. Hu¹, T. Hu¹, G. S. Huang^{1a}, X. T. Huang¹³, X. B. Ji[†], X. S. Jiang¹, X. Y. Jiang⁵, J. B. Jiao¹³, D. P. Jin¹, S. Jin¹, Yi Jin⁸, Y. F. Lai[†], G. Li[†], H. B. Li[†], H. H. Li[†], J. Li[†], R. Y. Li[†], S. M. Li[†], W. D. Li[†], W. G. Li[†], X. L. Li[†], X. N. Li[†], X. Q. Li^{†1}, Y. L. Li[†], Y. F. Liang¹⁴, H. B. Liao¹, B. J. Liu¹, C. X. Liu¹, F. Liu⁶, Fang Liu¹, H. H. Liu¹, H. M. Liu¹, J. Liu¹², J. B. Liu¹, J. P. Liu¹⁸, Q. Liu¹, R. G. Liu¹, Z. A. Liu¹, Y. C. Lou⁵, F. Lu¹, G. R. Lu⁵, J. G. Lu¹, C. L. Luo¹⁰, F. C. Ma⁹, H. L. Ma¹, L. L. Ma¹, Q. M. Ma¹, X. B. Ma⁵, Z. P. Ma¹, X. H. Mo¹, J. Nie¹, S. L. Olsen¹⁶, H. P. Peng^{17b}, R. G. Ping¹, N. D. Qi[†], H. Qi[†], J. F. Qiu¹, Z. Y. Ren¹, G. Rong¹, L. Y. Shan¹, L. Shang¹, C. P. Shen¹, D. L. Shen¹, X. Y. Shen¹, H. Y. Sheng¹, H. S. Sun¹, J. F. Sun¹, S. S. Sun¹, Y. Z. Sun¹, Z. J. Sun¹, Z. Q. Tan⁴, X. Tang¹, G. L. Tong¹, G. S. Vamer¹⁶, D. Y. Wang¹, L. Wang¹, L. L. Wang¹, L. S. Wang¹, M. Wang¹, P. Wang¹, P. L. Wang¹, W. F. Wang^{1c}, Y. F. Wang¹, Z. Wang¹, Z. Y. Wang¹, Zhe Wang¹, Zheng Wang², C. L. Wei[†], D. H. Wei[†], N. Wu¹, X. M. Xia¹, X. X. Xie¹, G. F. Xu¹, X. P. Xu⁶, Y. Xu¹¹, M. L. Yan¹⁷, H. X. Yang¹, Y. X. Yang³, M. H. Ye², X. Ye¹⁷, Z. Y. Yi[†], G. W. Yu¹, C. Z. Yuan¹, J. M. Yuan¹, Y. Yuan¹, S. L. Zang¹, Y. Zeng⁷, Yu Zeng¹, B. X. Zhang¹, B. Y. Zhang¹, C. C. Zhang¹, D. H. Zhang¹, H. Q. Zhang¹, H. Y. Zhang¹, J. W. Zhang¹, J. Y. Zhang¹, S. H. Zhang¹, X. M. Zhang¹, X. Y. Zhang¹³, Y. Yun Zhang¹⁴, Z. P. Zhang¹⁷, D. X. Zhao¹, J. W. Zhao¹, M. G. Zhao¹, P. P. Zhao¹, W. R. Zhao¹, Z. G. Zhao^{1d}, H. Q. Zheng¹², J. P. Zheng¹, Z. P. Zheng¹, L. Zhou¹, N. F. Zhou^{1d}, K. J. Zhu¹, Q. M. Zhu¹, Y. C. Zhu¹, Y. S. Zhu¹, Yingchun Zhu^{1b}, Z. A. Zhu¹, B. A. Zhuang¹, X. A. Zhuang¹, B. S. Zou¹

(BES Collaboration)

¹ Institute of High Energy Physics, Beijing 100049, People's Republic of China² China Center for Advanced Science and Technology (CCAST), Beijing 100080, People's Republic of China³ Guangxi Normal University, Guilin 541004, People's Republic of China⁴ Guangxi University, Nanning 530004, People's Republic of China⁵ Henan Normal University, Xinxiang 453002, People's Republic of China⁶ Huazhong Normal University, Wuhan 430079, People's Republic of China⁷ Hunan University, Changsha 410082, People's Republic of China⁸ Jinan University, Jinan 250022, People's Republic of China⁹ Liaoning University, Shenyang 110036, People's Republic of China¹⁰ Nanjing Normal University, Nanjing 210097, People's Republic of China¹¹ Nankai University, Tianjin 300071, People's Republic of China¹² Peking University, Beijing 100871, People's Republic of China¹³ Shandong University, Jinan 250100, People's Republic of China¹⁴ Sichuan University, Chengdu 610064, People's Republic of China¹⁵ Tsinghua University, Beijing 100084, People's Republic of China¹⁶ University of Hawaii, Honolulu, HI 96822, USA¹⁷ University of Science and Technology of China, Hefei 230026, People's Republic of China¹⁸ Wuhan University, Wuhan 430072, People's Republic of China¹⁹ Zhejiang University, Hangzhou 310028, People's Republic of China^a Current address: Purdue University, West Lafayette, IN 47907, USA^b Current address: DESY, D-22607, Hamburg, Germany^c Current address: Laboratoire de l'Accélérateur Linéaire, Orsay, F-91898, France^d Current address: University of Michigan, Ann Arbor, MI 48109, USA

Results are presented on $J = 0$ radiative decays to $\pi^+\pi^-$ and $\pi^0\pi^0$ based on a sample of 58M $J = 0$ events taken with the BES II detector. Partial wave analyses are carried out using the relativistic covariant tensor amplitude method in the 1.0 to 2.3 GeV/ c^2 mass range. There are conspicuous peaks due to the $f_2(1270)$ and two 0^{++} states in the 1.45 and 1.75 GeV/ c^2 mass regions. The first 0^{++} state has a mass of 1466^{+6}_{-20} MeV/ c^2 , a width of 108^{+14}_{-11} MeV/ c^2 , and a branching fraction $B(J = 0 \rightarrow f_0(1500) \rightarrow \pi^+\pi^-) = (0.67 \pm 0.02 \pm 0.28) \times 10^{-4}$. Spin 0 is strongly preferred over spin 2. The second 0^{++} state peaks at 1765^{+4}_{-3} MeV/ c^2 with a width of 145^{+8}_{-69} MeV/ c^2 . If this 0^{++} is interpreted as coming from $f_0(1710)$, the ratio of its branching fractions to $\pi^+\pi^-$ and K^+K^- is $0.41^{+0.11}_{-0.17}$.

PACS numbers: 12.39Mk, 13.25Gv, 14.40Cs

I. INTRODUCTION

QCD predicts the existence of glueballs, the bound states of gluons, and the observation of glueballs would provide a direct test of QCD. In the quenched approximation, lattice QCD calculations predict the lightest glueball to be a 0^{++} with the mass being in the region from 1.4 to 1.8 GeV/ c^2 [1]. Although the identification of a glueball is very complicated, there are several glueball candidates, including the $f_0(1500)$ and $f_0(1710)$. The properties of the $f_0(1500)$ and $f_0(1710)$ are reviewed in detail in the latest issue of the Particle Data Group (PDG) [2].

$J = 0$ radiative decays have been suggested as promising modes for glueball searches. The $J = 0 \rightarrow \pi^+\pi^-$ process was analyzed previously in the Mark III [3] and DM2 [4] experiments, in which there was evidence for $f_2(1270)$ and an additional $f_2(1720)$. However, the high mass shoulder of the $f_2(1270)$, at about 1.45 GeV/ c^2 , was unsettled. A revised amplitude analysis of Mark III data assigned the shoulder to be a scalar at 1.43 GeV/ c^2 , and, in addition, found the peak at 1.7 GeV/ c^2 to be scalar rather than tensor [5]. The $J = 0 \rightarrow \pi^0\pi^0$ process was also studied by the Crystal Ball [6] and BES I experiments [7], but no partial wave analysis has yet been performed on this channel. In this paper, the results of partial wave analyses on $J = 0 \rightarrow \pi^+\pi^-$ and $0 \rightarrow \pi^0\pi^0$ are presented based on a sample of 58M $J = 0$ events collected by the upgraded Beijing Spectrometer (BES II) located at the Beijing Electron Positron Collider (BEPC).

II. BES DETECTOR

BES II is a large solid-angle magnetic spectrometer that is described in detail in Ref. [8]. Charged particle momenta are determined with a resolution of $\frac{\Delta p}{p} = 1.78\% \sqrt{1 + p^2}$ (p in GeV/ c) in a 40-layer cylindrical main drift chamber (MDC). Particle identification is accomplished by specific ionization (dE/dx)

measurements in the drift chamber and time-of-flight (TOF) measurements in a barrel-like array of 48 scintillation counters. The dE/dx resolution is $\frac{\Delta dE}{dE} = 8.0\%$; the TOF resolution is $\Delta t_{TOF} = 180$ ps for Bhabha events. Outside of the time-of-flight counters is a 12-radiation-length barrel shower counter (BSC) comprised of gas tubes operating in limited stream mode. The BSC measures the energies of photons with a resolution of $\frac{\Delta E}{E} = 21\% \sqrt{E}$ (E in GeV). Outside the solenoidal coil, which provides a 0.4 T magnetic field over the tracking volume, is an iron yoke return that is instrumented with three double layers of counters that are used to identify muons.

In this analysis, a GEANT3 based Monte Carlo simulation program (SIMBES) [9] with detailed consideration of detector performance (such as dead electronic channels) is used. The consistency between data and Monte Carlo has been checked in many high purity physics channels, and the agreement is quite reasonable [9].

III. EVENT SELECTION

The first level of event selection of $J = 0 \rightarrow \pi^+\pi^-$ requires two charged tracks with total charge zero. Each charged track, reconstructed using MDC information, is required to be well fitted to a three-dimensional helix, be in the polar angle region $|\cos \theta_{MDC}| < 0.8$, and have the point of closest approach of the track to the beam axis be within 2 cm of the beam axis and within 20 cm from the center of the interaction region along the beam line.

More than one photon per event is allowed because of the possibility of fake photons coming from the interactions of charged tracks with the shower counter or from electronic noise in the shower counter. A neutral cluster is considered to be a photon candidate when the energy deposited in the BSC is greater than 50 MeV, the first hit is in the beginning six radiation lengths, the angle between the nearest charged track and the cluster is greater than 18° , and the angle be-

tween the cluster development direction in the BSC and the photon emission direction is less than 30° .

The total number of layers with hits associated with the two charged particles in the muon counter is required to be less than four in order to remove $\pi^+\pi^-$ events. To remove the large backgrounds from Bhabha events, we require that (i) the opening angle of the two tracks satisfies $\theta_{\text{op}} < 175^\circ$ and (ii) the energy deposit by each track in the BSC satisfies $E_{\text{SC}} < 1.0 \text{ GeV}$. We require $\theta_{\text{op}} > 10^\circ$ to remove conversions that occur at low $\pi^+\pi^-$ mass. In order to reduce the background from final states with kaons and electrons, both tracks are required to be identified as pions by TOF or dE/dx when the momenta are lower than $0.7 \text{ GeV}/c$. In other cases, at least one track is required to be identified as a pion by TOF.

Requirements on two variables, U and P_t^2 , are imposed [10]. The variable $U = (E_{\text{miss}} - \vec{P}_{\text{miss}} \cdot \hat{n})$ is required to satisfy $|U| < 0.15 \text{ GeV}$. Here, E_{miss} and \vec{P}_{miss} are, respectively, the missing energy and momentum of charged particles. The variable $P_t^2 = 4\vec{P}_{\text{miss}}^2 \sin^2 \theta = 2$ is required to be $< 0.0045 (\text{GeV}/c)^2$, where θ is the angle between the missing momentum and the photon direction. The U cut removes most background from events having multikaon or other neutral particles, such as $K(892)K$, K^+K^- events. The cut on P_t^2 is used to reduce backgrounds with π^0 s.

In order to reduce the dominant $\pi^+\pi^-$ background, events with more than one photon satisfying $M_{1,2}^0 < 0.065 \text{ GeV}/c^2$ are rejected. Here $M_{1,2}^0$ is the invariant mass of the two isolated photons with the smallest angle between the plane determined by these two photons and the direction of \vec{P}_{miss} in all possible photon combinations. $M_{1,2}^0$ is calculated using \vec{P}_{miss} and the angle between \vec{P}_{miss} and the π^0 direction. The advantage of this method is that it uses the momenta of the charged tracks measured by the MDC, which has good momentum resolution, and is independent of photon energy measurement.

Finally, the two charged tracks and photon in the event are kinematically fitted using four energy and momentum conservation constraints (4-C) under the $J = \pi^+\pi^-$ hypothesis to obtain better mass resolution and to suppress backgrounds further by using the requirements $\chi^2_{\text{min}} < 15$ and $\chi^2_{\text{min}} < 2_{K^+K^-}$. If there is more than one photon, the fit is repeated using all permutations and the combination with the best fit to $\pi^+\pi^-$ is retained.

For $J = \pi^+\pi^-$, the π^0 mesons in the event are identified through the decay $\pi^0 \rightarrow \gamma\gamma$. The isolated photon is required to have the energy deposited in

the BSC greater than 80 MeV and come from the interaction point. The number of isolated photons is required to be greater than four and less than seven. A 4-C kinematic fit to $J = \pi^+\pi^-$ is performed, the combination of π^0 photons with the smallest χ^2 is selected, and a kinematic fit $\chi^2_{\text{min}} < 15$ is required. For π^0 photons, there are 15 combinations from which to construct two π^0 s. To select π^0 s, we choose the combination with the smallest χ^2 , where $\chi^2 = \frac{(\vec{M}_{1,2} - \vec{M}_{\pi^0})^2 + (\vec{M}_{3,4} - \vec{M}_{\pi^0})^2}{M_{1,2}^0 M_{3,4}^0}$ and require $M_{1,2}^0 M_{3,4}^0 < 40 (\text{MeV}/c^2)^2$. To reduce background with π^0 s, events with the invariant mass of a π^0 and one photon in the π^0 mass interval $M_{1,2}^0 M_{\pi^0} < 30 (\text{MeV}/c^2)^2$ are rejected. To further suppress backgrounds with more than one neutral particle recoiling to the $\pi^+\pi^-$ system, the recoiling mass squared of the $\pi^+\pi^-$ system is required to be less than $4.8 (\text{GeV}/c^2)^2$.

Figure 1 shows the $\pi^+\pi^-$ mass spectrum for the selected events, together with the corresponding background distribution and the Dalitz plot. There is a strong $\pi^0(770)$ peak due to background from $J = \pi^+\pi^-$. A strong $f_2(1270)$ signal, a shoulder on the high mass side of the $f_2(1270)$, an enhancement at $1.7 \text{ GeV}/c^2$, and a peak at $2.1 \text{ GeV}/c^2$ are clearly present over the $\pi^+\pi^-$ background. The shaded histogram corresponds to the Monte Carlo simulated $J = \pi^+\pi^-$ background distribution.

Fig. 2 shows the $\pi^0\pi^0$ mass spectrum for selected events. The shaded histogram shown in Fig. 2 corresponds to a sum of Monte Carlo simulated background events using PDG branching ratios [2]. The peak below $0.5 \text{ GeV}/c^2$ is mainly from $J = \pi^+\pi^-$; $\pi^0\pi^0$; $3\pi^0$; $\pi^0\pi^+\pi^-$. In general, the $\pi^+\pi^-$ and $\pi^0\pi^0$ mass spectra exhibit similar structures above $1.0 \text{ GeV}/c^2$.

IV. PARTIAL WAVE ANALYSIS

We have carried out partial wave analyses for the mass range from 1.0 to $2.3 \text{ GeV}/c^2$ using relativistic covariant tensor amplitudes constructed from Lorentz-invariant combinations of the polarization and momentum 4-vectors of the initial and final state particles, with helicity ± 1 for $J = \pi^+\pi^-$ initial states [11]. Cross sections are summed over photon polarizations. The relative magnitudes and phases of the amplitudes are determined by a maximum likelihood fit.

For $J = \pi^+\pi^-$, the following channels are fitted to the data:

$$J = \pi^+\pi^- \quad f_2(1270)$$

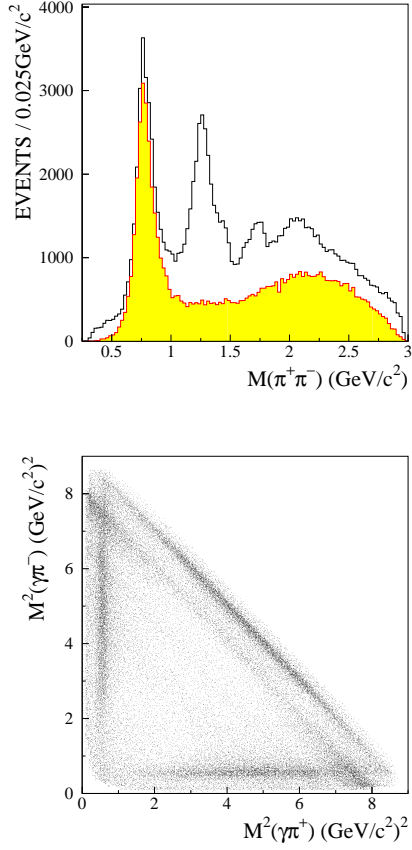


FIG . 1: Invariant mass spectrum of $\pi^+\pi^-$ and the Dalitz plot for $J=1^+$, where the shaded histogram in the upper panel corresponds to the estimated backgrounds.

- ! $f_0(1500)$
- ! $f_0(1710)$
- ! $f_2(1810)$
- ! $f_0(2020)$
- ! $f_2(2150)$
- ! $f_4(2050)$:

Constant width Breit-Wigner functions are used for each resonance. The form is described as follows:

$$BW_X = \frac{m}{s - m^2 + im};$$

where s is the square of $\pi^+\pi^-$ invariant mass, m and Γ are the mass and width of intermediate resonance X , respectively.

The dominant background in $J=1^+\pi^+\pi^-$ comes from $J=1^+\pi^+\pi^0$. From Mark III's analysis on $J=1^+\pi^+\pi^0$, described in terms of the amplitudes representing the sequential two-body decay process $J=1^+ \rightarrow \pi^+\pi^0$; [12], a complete description of the

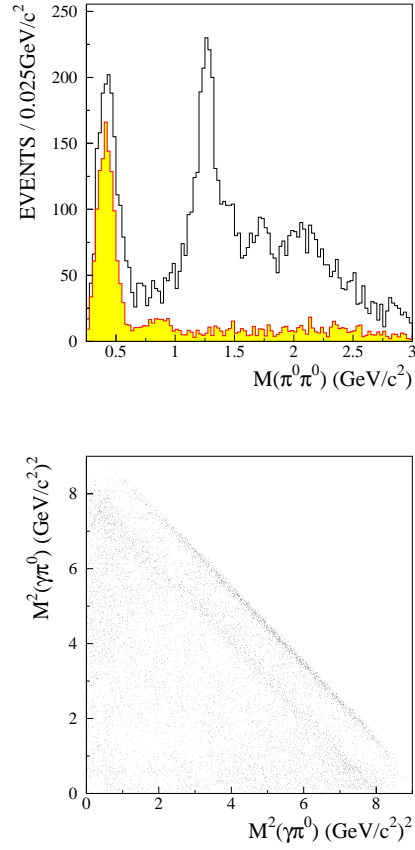


FIG . 2: Invariant mass spectrum of $\pi^0\pi^0$ and the Dalitz plot for $J=1^+$, where the shaded histogram in the upper panel corresponds to the estimated backgrounds.

data requires not only the dominant (770) , but also contributions from excited states of (770) . Using the generator based on the results of Ref. [12] and the new branching fraction measurement of BES II [13], $J=1^+\pi^+\pi^0$ events are generated and given the opposite log likelihood in the fit to cancel the background events in the data.

Due to the limitation of the present statistics and the complexity of the large background, it is difficult to cleanly distinguish components in the high mass region. The main goal of this analysis will be to understand the structures below $2.0 \text{ GeV}/c^2$. We use the four states $f_2(1810)$, $f_0(2020)$, $f_2(2150)$, and $f_4(2050)$, which are listed in PDG [2] in the fit with the masses and widths fixed to those in the PDG, to describe the contribution of the high mass states in the mass range below $2.0 \text{ GeV}/c^2$.

For the 2^{++} states, relative phases between different helicity amplitudes for a single resonance are theoretically expected to be very small [14]. Therefore, these relative phases are set to zero in the final fit so as to

constrain the intensities further.

After the mass and width optimization, the resulting fitted intensities are illustrated in Figs. 3 and 4. Angular distributions in the whole mass range are shown in Fig. 5. Here, θ is the polar angle of the photon in the J/ψ rest frame, and θ^* is the polar angle of the pion in the $\psi(2S)$ rest frame.

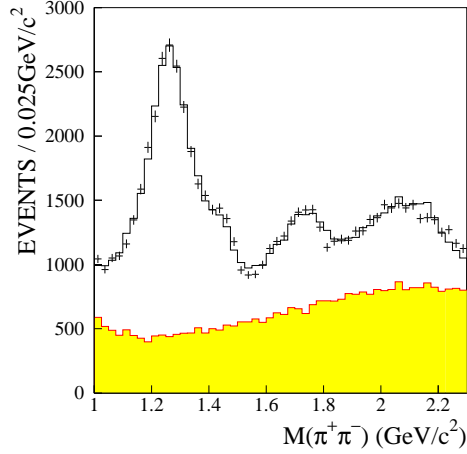


FIG. 3: The $\psi(2S)$ invariant mass distribution from $J/\psi \rightarrow \pi^+ \pi^-$. The crosses are data, the full histogram shows the maximum likelihood fit, and the shaded histogram corresponds to the $\psi(2S)$ background.

From Figs. 3 and 5, we see that the fit agrees well with data. Fig. 4 shows the distributions of the individual components and full 0^{++} and 2^{++} contributions including interferences. A fit to $f_2(1270)$ gives a fitted mass of 1262^{+1}_{-2} MeV/ c^2 and a width of 175^{+6}_{-4} MeV/ c^2 . The fitted masses and widths of the $f_0(1500)$ and $f_0(1710)$ are $M_{f_0(1500)} = 1466 \pm 6$ MeV/ c^2 , $\Gamma_{f_0(1500)} = 108^{+14}_{-11}$ MeV/ c^2 and $M_{f_0(1710)} = 1765^{+4}_{-3}$ MeV/ c^2 , $\Gamma_{f_0(1710)} = 145 \pm 8$ MeV/ c^2 , respectively. The branching fractions of $f_2(1270)$, $f_0(1500)$, and $f_0(1710)$ determined by the partial wave analysis fit are $B(J/\psi \rightarrow f_2(1270) \rightarrow \pi^+ \pi^-) = (9.14 \pm 0.07) \times 10^{-4}$, $B(J/\psi \rightarrow f_0(1500) \rightarrow \pi^+ \pi^-) = (6.65 \pm 0.21) \times 10^{-5}$, and $B(J/\psi \rightarrow f_0(1710) \rightarrow \pi^+ \pi^-) = (2.64 \pm 0.04) \times 10^{-4}$, respectively. For the $f_2(1270)$, we find the ratios of helicity amplitudes $x = 0.89 \pm 0.02$ and $y = 0.46 \pm 0.02$ with correlation factor $\rho = 0.26$, where $x = A_1/A_0$, $y = A_2/A_0$, $A_{0;1;2}$ are the helicity amplitudes. The errors here are statistical errors. An alternative fit is tried by replacing $f_0(1500)$ with a 2^{++} resonance. There are three helicity amplitudes fitted for spin 2, while only one amplitude for spin 0, which means the the number of degrees of freedom is increased by 2 in the $J^P = 2^+$ case. However, the log likelihood is worse by 108.

This indicates that $f_0(1500)$ with $J^P = 0^+$ is strongly favored. If the $f_0(1710)$ is removed from the fit, the log likelihood is worse by 379, which corresponds to a signal significance much larger than 5.

The partial wave analysis of $J/\psi \rightarrow \pi^0 \pi^0$ is performed independently. The components used are the same as those of $J/\psi \rightarrow \pi^+ \pi^-$. Due to the limited statistics, we take the partial wave analysis results of $J/\psi \rightarrow \pi^0 \pi^0$ as a cross-check of the ones obtained in the charged channel. The background distribution is close to flat in the mass interval 1.0 – 2.3 GeV/ c^2 , so we use $1-p_2(m)$ multiplied by phase space to approximately describe such a flat contribution, where the 2nd order polynomial function $p_2(m)$ is obtained by fitting the $\pi^0 \pi^0$ mass phase space distribution of $J/\psi \rightarrow \pi^0 \pi^0$ Monte Carlo simulation.

The fitted intensities as a function of $\pi^0 \pi^0$ mass are illustrated in Fig. 6. A fit to $f_2(1270)$ gives a fitted mass of 1261 ± 6 MeV/ c^2 and a width of 188^{+18}_{-16} MeV/ c^2 . The fitted masses and widths of the $f_0(1500)$ and $f_0(1710)$ are $M_{f_0(1500)} = 1485 \pm 21$ MeV/ c^2 , $\Gamma_{f_0(1500)} = 178^{+60}_{-40}$ MeV/ c^2 and $M_{f_0(1710)} = 1755 \pm 14$ MeV/ c^2 , $\Gamma_{f_0(1710)} = 155^{+30}_{-26}$ MeV/ c^2 , respectively. The errors shown here are statistical.

Besides the above global fit, a bin-by-bin fit is applied to $J/\psi \rightarrow \pi^+ \pi^-$ data using the method described in Ref. [15]. A strong $f_2(1270)$ is observed, and the S-wave $\pi^+ \pi^-$ mass distribution shows a large signal at 1.45 GeV/ c^2 , a significant signal at 1.75 GeV/ c^2 , and a peak at 2.1 GeV/ c^2 . In general, the bin-by-bin fit gives similar features as those of the global fit, and the results of these two fits are approximately consistent with each other.

V. SYSTEMATIC ERRORS

The systematic errors for the partial wave analysis fit to $J/\psi \rightarrow \pi^+ \pi^-$ data are estimated by varying the masses and widths of the $f_2(1270)$, $f_0(1500)$, and $f_0(1710)$ within the fitted errors; varying the masses and widths of the $f_2(1810)$, $f_0(2020)$, $f_2(2150)$, and $f_4(2050)$ within the PDG errors [2]; adding a small component $f_2(1565)$; varying the background component within reasonable limits; and replacing the $f_2(1810)$ with the $f_2(1950)$. They also include the uncertainties in the number of J/ψ events analyzed, the efficiency of photon detection, the efficiency of MDC tracking, and the kinematic fit. The systematic errors for the global fit are summarized in Table I.

For the $f_2(1270)$, the total systematic errors are 0.10 and 0.17 for x and y , respectively. The correlation factor between the x and y systematic errors is

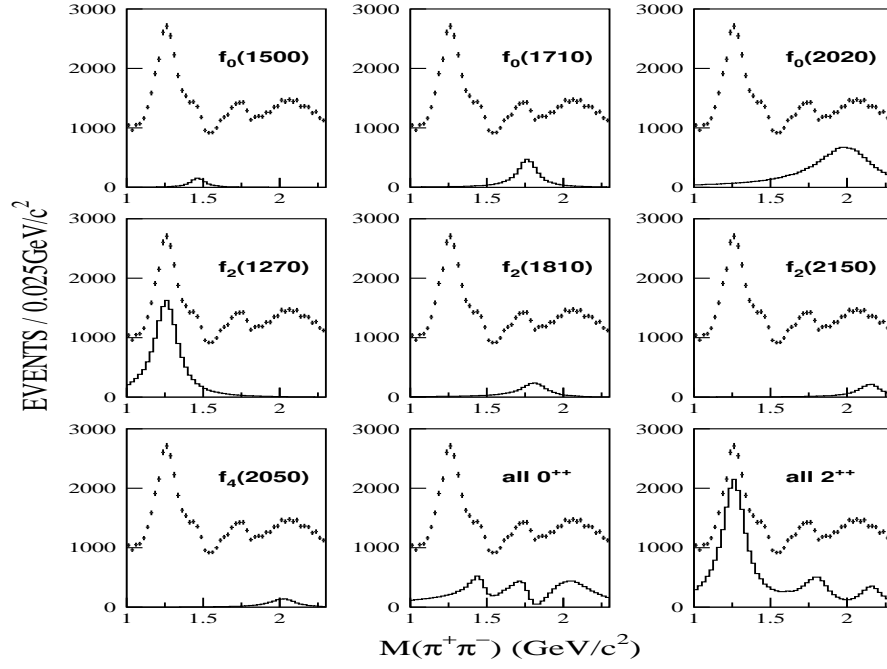


FIG. 4: The mass projections of the individual components for $J = 0^{++}$. The crosses are data. The complete 0^{++} and 2^{++} contributions are also shown, including all interferences.

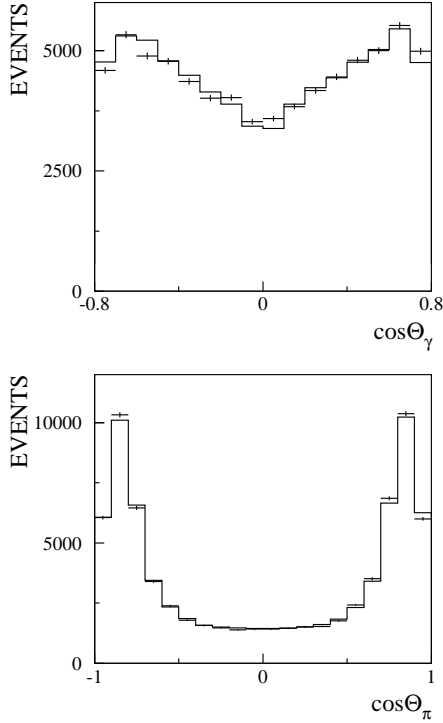


FIG. 5: Projections in $\cos \Theta_\gamma$ and $\cos \Theta_\pi$ for the whole mass range. The crosses are data ($J = 0^{++}$ sample), and the histograms are the fit results.

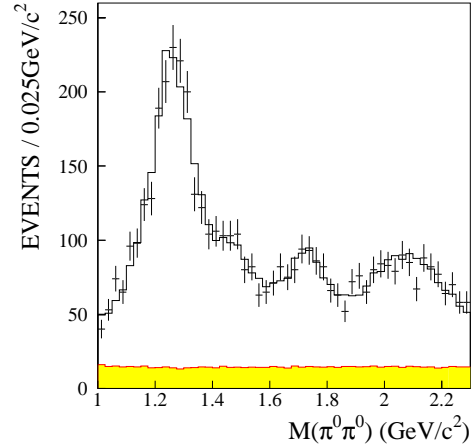


FIG. 6: The $\pi^0\pi^0$ invariant mass distribution from $J = 0^{++}$. The crosses are data, the full histogram shows the maximum likelihood fit, and the shaded histogram corresponds to the background.

0.29 which is calculated with $\chi^2 = \sum_i \frac{(x_i - y_i)^2}{\sigma_i^2}$, where i runs over all systematic errors.

Table II shows the mass, width, and branching fraction measurements for $f_2(1270)$, $f_0(1500)$, and $f_0(1710)$, where the first error is statistical and the second is systematic, determined by adding all sources

in quadrature. In order to compare the branching fractions of $f_2(1270)$, $f_0(1500)$, and $f_0(1710)$ in $^{0+}$ and $^{0-}$, we extract the mass and width of each component in $^{0-}$ to those of the charged channel and re-calculate the branching fractions and estimate the systematic errors. The results are shown in Table III. The branching fractions determined from the two channels agree with each other within errors after considering isospin corrections.

VI. DISCUSSION

The measured mass of the $f_2(1270)$, 1262^{+1}_{-7} MeV/ c^2 , is lower than the PDG value, and the branching fraction of $J=1^-$ $f_2(1270)$; $f_2(1270) \rightarrow \pi^+\pi^-$ is a bit higher than the PDG value [2]. A fit with the PDG mass and width is visibly poorer, and the log likelihood is worse than the optimum fit by 44. In this analysis, the S-wave contribution on the high mass shoulder of the large $f_2(1270)$ peak is well separated, which may explain this mass difference. The ratios of the helicity amplitudes of the $f_2(1270)$ from the present analysis are $x = 0.89 \pm 0.02 \pm 0.10$ and $y = 0.46 \pm 0.02 \pm 0.17$ with correlation $\text{stat} = 0.26$ and $\text{sys} = 0.29$. The values of x and y are in agreement with predictions [4, 16] within the errors. Comparing to the results determined by DM2 [4], Mark III [3], and Crystal Ball [17], there is a difference in the value of y . The main reason for this difference may be that we consider interferences from other states in the 1.0 to 2.3 GeV/ c^2 mass range, while previous analyses by DM2 and Mark III ignored these and only considered the $f_2(1270)$ in the 1.15–1.4 GeV/ c^2 mass range.

The most remarkable feature of the above results is that three 0^{++} states at the mass 1.45, 1.75, and 2.1 GeV/ c^2 are observed from the partial wave analysis. For the high mass state at 2.1 GeV/ c^2 , we use the $f_0(2020)$, which is listed in the PDG, to describe it. No further efforts are made on the measurements of its resonant parameters due to the difficulties described in Section IV.

The lower 0^{++} state peaks at a mass of 1466 ± 20 MeV/ c^2 with a width of $108^{+14}_{-11} \pm 21$ MeV/ c^2 , which is consistent with the scalar glueball candidate, $f_0(1500)$. Spin 0 is strongly preferred over spin 2. Therefore we interpret the small but definite shoulder on the high mass side of the $f_2(1270)$ in the $^{0+}$ mass distribution as originating from the $f_0(1500)$, which interferes with nearby resonances in the partial wave analysis. However, due to the uncertainties of the mass and width determinations and large interferences between the S-wave states, the existence

of the $f_0(1370)$ in $J=1^-$ cannot be excluded by present data.

Strong production of the $f_0(1710)$ was observed in the partial wave analysis of $J=1^-$ KK , with a mass of $1740 \pm 4^{+10}_{-25}$ MeV/ c^2 , a width of 166^{+5+15}_{-8-10} MeV/ c^2 , and a branching fraction of $J=1^-$ $f_0(1710)$; $f_0(1710) \rightarrow \pi^+\pi^-$ of $(9.62 \pm 0.29^{+2.11+2.81}_{-1.86-0.00}) \times 10^{-4}$ [15]. Interpreting the 0^{++} state in the mass region 1.75 GeV/ c^2 as coming from the $f_0(1710)$ and using the branching fraction of $f_0(1710) \rightarrow \pi^+\pi^-$ determined from $f_0(1710) \rightarrow \pi^+\pi^-$ after isospin correction and the branching fraction of $f_0(1710) \rightarrow KK$ in Ref. [15], we obtain the ratio of $f_0(1710) \rightarrow \pi^+\pi^-$ to KK branching fractions for the $f_0(1710)$ as

$$\frac{(f_0(1710) \rightarrow \pi^+\pi^-)}{(f_0(1710) \rightarrow KK)} = 0.41^{+0.11}_{-0.17}.$$

The ratio is consistent with the PDG value $(0.200 \pm 0.024 \pm 0.036)$ [2] within the errors. An alternative interpretation for this 0^{++} state is the $f_0(1790)$. Data on $J=1^-$ $\pi^+\pi^-$ and K^+K^- show a definite peak in $\pi^+\pi^-$ at 1790 MeV/ c^2 but no significant signal in K^+K^- [18]. If the mass and width of the 0^{++} state are fixed to 1790 MeV/ c^2 and 270 MeV/ c^2 found in [18], the log likelihood is worse by 47. This 0^{++} state may also be a superposition of $f_0(1710)$ and $f_0(1790)$.

Due to the uncertainty of the high mass region, we do an alternative fit removing the $f_4(2050)$ and re-optimizing the masses and widths of $f_2(1270)$, $f_0(1500)$, and $f_0(1710)$ for the $J=1^-$ $\pi^+\pi^-$ sample. The log likelihood is worse by 160. The fit gives a $f_2(1270)$ mass of $1259 \pm 2 \pm 6$ MeV/ c^2 and a width of $175^{+4}_{-5} \pm 8$ MeV/ c^2 . The measured masses and widths of the $f_0(1500)$ and $f_0(1710)$ are $M_{f_0(1500)} = 1466 \pm 6 \pm 17$ MeV/ c^2 , $\Gamma_{f_0(1500)} = 118^{+14}_{-15} \pm 28$ MeV/ c^2 and $M_{f_0(1710)} = 1768^{+5}_{-4} \pm 15$ MeV/ c^2 , $\Gamma_{f_0(1710)} = 112^{+10}_{-8} \pm 52$ MeV/ c^2 , respectively. The branching fractions of the $f_2(1270)$, $f_0(1500)$, and $f_0(1710)$ are $B(J=1^- f_2(1270) \rightarrow \pi^+\pi^-) = (9.04 \pm 0.07 \pm 0.89) \times 10^{-4}$, $B(J=1^- f_0(1500) \rightarrow \pi^+\pi^-) = (0.68 \pm 0.02 \pm 0.28) \times 10^{-4}$, and $B(J=1^- f_0(1710) \rightarrow \pi^+\pi^-) = (1.40 \pm 0.03 \pm 0.55) \times 10^{-4}$, respectively.

The light-meson spectroscopy of scalar states in the mass range 1–2 GeV/ c^2 , which has long been a source of controversy, is still very complicated. Overlapping states interfere with each other differently in different production and decay channels. More experimental data are needed to clarify the properties of these scalar states.

TABLE I: Estimation of systematic errors for the $J = 1^-$ in the global fit. Masses and widths are in MeV/c^2 . x and y are the ratios of helicity amplitudes. ρ is the correlation factor between x and y .

	$f_2(1270)$						$f_0(1500)$			$f_0(1710)$		
	M	B (%)	x (%)	y (%)	ρ		M	B (%)		M	B (%)	
M and ρ of $f_2(1270)$		1.4	0.2	2.0	0.26		0	0	2.3	0	0	0.1
M and ρ of $f_0(1500)$	1	0	0.1	0.1	2.2	0.26		10.1		0	1	1.9
M and ρ of $f_0(1710)$	0	0	0.1	0.5	0.6	0.26	0	1	2.6			8.9
M and ρ of $f_2(1810)$	0	1	1.4	2.9	0.5	0.26	1	7	4.2	3	15	6.9
M and ρ of $f_0(2020)$	1	3	1.0	1.6	1.2	0.27	6	2	3.0	5	10	5.8
M and ρ of $f_2(2150)$	1	2	1.2	1.2	0.4	0.26	3	0	3.2	1	3	3.3
M and ρ of $f_4(2050)$	0	1	0.1	0.4	0.7	0.26	1	2	0.4	0	0	0.7
add $f_2(1565)$	2	5	0.2	6.9	34.6	0.35	3	7	18.6	3	10	2.9
MDC tracking and kinematic fit	4	4	3.5	6.2	12.8	0.38	14	18	31.0	8	1	13.4
+ 10 %	3	2	1.8	3.4	4.3	0.33	4	2	13.9	3	10	7.8
replace $f_2(1810)$ with $f_2(1950)$	4	5	8.7	2.1	4.4	0.27	12	4	11.0	5	65	16.4
$N_{J=1^-}$			4.7						4.7			4.7
Detection efficiency of photon			2.0						2.0			2.0
Total Systematic error	7	9	11.1	10.7	37.6	0.29	20	21	42.4	12	69	26.8

TABLE II: Fit results for $J = 1^-$. The first error is statistical, and the second is systematic.

$J = 1^-$ $X; X \rightarrow 0^+ 0^+$									
	Mass (MeV/c^2)			Γ (MeV/c^2)			B (10^{-4})		
$f_2(1270)$	1262 $^{+1}_{-2}$	7		175 $^{+6}_{-4}$	9		9.14	0.07	1.01
$f_0(1500)$	1466	6	20	108 $^{+14}_{-11}$	21		0.67	0.02	0.28
$f_0(1710)$	1765 $^{+4}_{-3}$	12		145	8	69	2.64	0.04	0.71

TABLE III: The branching fraction measurements of $J = 1^- \rightarrow 0^+ 0^+$, where the masses and widths of the resonances are fixed to the values determined from $J = 1^-$. The first error is statistical, and the second is systematic.

$J = 1^-$ $X; X \rightarrow 0^+ 0^+$									
	Mass (MeV/c^2)			Γ (MeV/c^2)			B (10^{-4})		
$f_2(1270)$	same as charged channel			4.00			0.09	0.58	
$f_0(1500)$	same as charged channel			0.34			0.03	0.15	
$f_0(1710)$	same as charged channel			1.33			0.05	0.88	

VII. SUMMARY

In summary, the partial wave analyses of $J = 1^-$ and $J = 1^- \rightarrow 0^+ 0^+$ using 58M $J = 1^-$ events of BES II show strong production of $f_2(1270)$ and evidence for two 0^{++} states in the 1.45 and 1.75 GeV/c^2 mass regions. For the $f_2(1270)$, the branching ratio determined by the partial wave analysis is $B(J = 1^- \rightarrow f_2(1270) \rightarrow 0^+ 0^+) = (9.14 \pm 0.07 \pm 1.01) \times 10^{-4}$. The ratios of the helicity amplitudes of the $f_2(1270)$ are determined to be $x = 0.89 \pm 0.02 \pm 0.10$ and $y = 0.46 \pm 0.02 \pm 0.17$ with correlations $\rho_{\text{stat}} = 0.26$ and $\rho_{\text{sys}} = 0.29$. The $f_0(1500)$ has a mass of $1466 \pm 6 \pm 20 \text{ MeV}/c^2$, a width of $108^{+14}_{-11} \pm 21 \text{ MeV}/c^2$, and a branching frac-

tion $B(J = 1^- \rightarrow f_0(1500) \rightarrow 0^+ 0^+) = (0.67 \pm 0.02 \pm 0.28) \times 10^{-4}$. The 0^{++} state in the 1.75 GeV/c^2 mass region has a mass of $1765^{+4}_{-3} \pm 12 \text{ MeV}/c^2$ and a width of $145 \pm 8 \pm 69 \text{ MeV}/c^2$. If this 0^{++} state is interpreted as coming from $f_0(1710)$, the ratio of the $f_0(1710) \rightarrow KK$ branching fractions is $0.41^{+0.11}_{-0.17}$. This may help in understanding the properties of $f_0(1500)$ and $f_0(1710)$.

VIII. ACKNOWLEDGMENTS

The BES collaboration thanks the staff of BEPC and computing center for their hard efforts. We wish to thank Prof. David Bugg for contributions to the

early stage of this analysis. This work is supported in part by the National Natural Science Foundation of China under contracts Nos. 10491300, 10225524, 10225525, 10425523, the Chinese Academy of Sciences under contract No. KJ 95T-03, the 100 Talents Program of CAS under Contract Nos. U-11, U-24, U-

25, and the Knowledge Innovation Project of CAS under Contract Nos. KJCX2-SW-N10, U-602, U-34 (IHEP), the National Natural Science Foundation of China under Contract No. 10225522 (Tsinghua University), and the Department of Energy under Contract No. DE-FG02-04ER41291 (U Hawaii).

-
- [1] G. Bali, K. Schilling, A. Hulsebos, A. Irving, C. Michael, and P. Stephenson, Phys. Lett. B 309, 378 (1993); C. Michael, Hadron Spectroscopy, AIP Conf. Proc. No. 432 (AIP, Melville, NY, 1997), p. 657; W. Lee, and D. Weinarten, hep-lat/9805029; C. J. Morningstar, and M. Peardon, Phys. Rev. D 60, 034509 (1999).
 - [2] Particle Data Group, S. Eidelman et al., Phys. Lett. B 592, 1 (2004).
 - [3] R. M. Baltrusaitis et al., Phys. Rev. D 35, 2077 (1987).
 - [4] J. E. Augustin et al., Zeit. Phys. C 36, 369 (1987).
 - [5] W. Dunwoodie, Hadron Spectroscopy, AIP Conf. Proc. No. 432 (AIP, Melville, NY, 1997), p. 753.
 - [6] L. Kopke, N. Wermes, Phys. Rep. 174, 67 (1989).
 - [7] J. Z. Bai et al., (BES Collaboration), Phys. Rev. Lett. 81, 1179 (1998).
 - [8] J. Z. Bai et al., (BES Collaboration), Nucl. Phys. A 458, 627 (2001).
 - [9] M. Ablikim, et al., (BES Collaboration), Nucl. Instrum. Meth. A 552, 344 (2005).
 - [10] T. H. Ine et al., Phys. Lett. 45, 1146 (1980).
 - [11] B. S. Zou and D. V. Bugg, Eur. Phys. J. A 16, 537 (2003).
 - [12] L. P. Chen and W. Dunwoodie, SLAC-PUB-5674 (1991).
 - [13] J. Z. Bai et al., (BES Collaboration), Phys. Rev. D 70, 012005 (2004).
 - [14] J. G. Komer, J. H. Kuhn, and H. Schneider, Phys. Lett. B 120, 444 (1983).
 - [15] J. Z. Bai et al., (BES Collaboration), Phys. Rev. D 68, 052003 (2003).
 - [16] M. Krammer, Phys. Lett. B 74 361 (1978).
 - [17] C. Edwards et al., Phys. Rev. D 25, 3065 (1982).
 - [18] M. Ablikim, et al., (BES Collaboration), Phys. Lett. B 607, 243 (2005).